PHYSICAL REVIEW C VOLUME 11, NUMBER 2 FEBRUARY 1975

Consequences of fission deexcitation of compound nuclei formed in heavy-ion reactions

F. Plasil
Physics Division, Oak Ridge National Laboratory, Oak Ridge, Tennessee 37830*

M. Blann†
Department of Chemistry and Nuclear Structure Research Laboratory, University of Rochester, Rochester, New York 14627
(Received 13 May 1974)

Restrictions on cross sections of compound nuclei surviving fission during the deexcitation process are investigated for a variety of heavy-ion projectile-target combinations. Calculations are performed within the framework of the Bohr-Wheeler model using angular-momentum-dependent fission barriers calculated from the rotating liquid drop model of Cohen, Plasil, and Swiatecki. It is shown that fission severely limits the cross sections of evaporation residue products at higher bombarding energies, that the critical angular momenta of such a model slowly increase with increasing bombarding energy, and that these critical angular momenta are very much lower than the values at which the fission barrier is thought to disappear. Calculated cross sections are in reasonable agreement with several experimental excitation functions. Experimental results are also compared with limits on fusion cross sections resulting from entrance conditions and comparisons are made between the consequences of the two types of models—entrance condition limits and fission-imposed limits on evaporation residue products.

[NUCLEAR REACTIONS Calculated evaporation residue $\sigma(E)$. HI projectiles ^{11}B to ^{84}Kr, targets ^{10}B to ^{165}Ho, compound nuclei ^{43}Sc to ^{211}Ac, $E = 3.5$–10.5 MeV/nucleon. Deduced critical J.]

I. INTRODUCTION

With the advent of a new generation of heavy-ion accelerators, fundamental questions are being raised about effects that govern interactions of very heavy ions with target nuclei. Under what conditions will an interacting target and projectile hold together sufficiently long to form a compound nucleus? How do the target and projectile charge, relative energy, and angular momentum enter into the resolution of this question? Once formed, what is the destiny of the compound nuclei, some of which may have very high angular momenta?

Existing experimental measurements which may give some indication of answers to these questions involve measurements of evaporation residue cross sections σ_{er} and fission cross sections σ_f. The sum of σ_{er} and σ_f in any given case is equal to the compound nucleus cross section σ_{cn} provided that it is possible to assume that all observed fission products result from an equilibrated (compound) system. The extent to which this assumption is valid is still an open question.

Experimental results have often been interpreted in terms of a critical angular momentum above which it is assumed that compound nucleus formation will not take place. Often the experimental cross sections which were analyzed by this convenient sharp cutoff approximation were evaporation residue cross sections rather than compound nucleus formation cross sections. The σ_{er} may be limited by several physically different processes. One type of limit is related to whether or not a compound nucleus can be formed for a given impact parameter, energy, and choice of target and projectile. The nature of such a limit on compound nucleus formation is not yet fully understood, and nomenclature for this type of limit varies. In this work we shall refer to limits on the formation probability of compound nuclei as "entrance condition limits." Other terms that have been used to describe limits on compound nucleus formation or on complete fusion are "entrance channel limits" and "contact configuration limits." The other important limit on σ_{er} is due to fission of high angular momentum states during the deexcitation of the compound and daughter nuclei.[1] The relative importance of these two types of limits on σ_{er} is not well established at present and remains a challenge for the future to both experimentalists and theoreticians.

In this paper, we shall consider primarily the angular momentum limit due to fission. The fission mode of deexcitation is particularly important in heavy-ion reactions because the fission barrier B_f decreases rapidly with increasing

angular momentum. Cohen, Plasil, and Swiatecki[2] (CPS) have calculated the variation of B_f with angular momentum in the rotating liquid drop model. We have taken the results of Ref. 2 and have applied them in a calculation that includes fission as one of the competing modes of compound-nucleus deexcitation. The angular momentum limits predicted by our calculation may be approximated (in the sharp cutoff approximation) by critical values of angular momentum J^{f}_{crit}. This fission-imposed critical value of J can be compared with J_{crit} values extracted from σ_{er} measurements only if J^{ec}_{crit} is greater than J^{f}_{crit}, where J^{ec}_{crit} is an analogous critical value of angular momentum imposed by entrance conditions. Thus we shall explore here the application of the CPS rotating liquid drop model to calculations of evaporation residue cross sections. We shall make comparisons with experimental results and shall study the sensitivity of the calculations to changes in parameters and to various approximations. For the purpose of completeness, we shall consider alternative limits on σ_{er} (involving different J_{crit} values) and how these limits relate to our fission limit. The various terms for cross sections and for critical values of angular momentum which will be used throughout the text are given in Table I.

The general organization of this work is as follows. In Sec. II A, a brief description of the rotating liquid drop model (which will be used to calculate ground-state and saddle-point rotational energies) is given. Section II B will then describe how the rotating drop model is used in a multiple-particle-emission computer code to predict limits on fission cross sections in the evaporation cascade. Results of calculations will be presented in Sec. II C in order to indicate how and when fission may be expected to impose the limit on σ_{er}, and comparisons will be made with entrance condition limits. In Sec. II D we will discuss the effects of variation of parameters which are not known accurately, such as the ratio of saddle-point to equilibrium-deformed single-particle level densities, the fission barrier, and the amount of angular momentum removed by particle emission. Results illustrating the importance of considering more than just first-chance particle emission vs fission competition will also be shown. In Sec. III, some further comparisons will be made with models which predict a limit on σ_{cn} due to entrance conditions, and in Sec. IV comparisons will be presented between calculated and experimental results for σ_{er} and σ_{cn} values.

TABLE I. Definition of terms.

σ_{cn}	Compound nucleus cross section
σ_{er}	Cross section for evaporation residue products
σ_f	Fission cross section
σ_r	Total reaction cross section
σ_j	Partial reaction cross section for angular momentum J
J^{cn}_{crit}	Critical angular momentum for the formation of a compound nucleus
J^{er}_{crit}	Critical angular momentum for evaporation residue products
J^{f}_{crit}	Critical angular momentum for evaporation residue products due to fission competition (obtained from our calculations)
J^{ec}_{crit}	Critical angular momentum due to entrance conditions (see text for description)
B_f	Fission barrier
$J(B_f=0)$	Angular momentum at which the fission barrier is zero

II. METHOD OF CALCULATION

A. Rotating liquid drop model

A detailed description of the rotating liquid drop model is given in Ref. 2 and we give only a brief description. The model considers configurations of a rotating uniformly charged fluid endowed with a surface tension and having a sharp boundary. The effective potential energy of the rotating liquid drop from which configurations of equilibrium were obtained by differentiation is given by $E=E_s+E_c+E_r$, where E_s is the surface energy, E_c is the electrostatic energy, and E_r is the rotational energy. The surface energy was taken to be equal to the surface area of the configuration under consideration multiplied by the surface energy coefficient; the Coulomb energy is the sum of interactions between pairs of volume elements interacting according to an inverse-distance potential, and the rotational energy was taken as the square of the angular momentum divided by twice the moment of inertia of the drop configuration. The moment of inertia was taken to be that of a rigid body and thus the configurations were confined to gyrostatic equilibrium with all fluid elements in uniform rotation about a common axis. Configurations of equilibrium that were studied were given by the condition that $\delta E=0$ for all small variations in the degrees of freedom specifying the system. The system was parametrized in terms of Legendre polynomials as described in Ref. 3. Equilibrium configurations were obtained in terms of two dimensionless parameters x and y, where x is the fissility parameter given by the ratio of the Coulomb energy of a sphere to twice its surface energy, and y is the rotational parameter, given by the ratio of the rotational energy of a sphere to its surface energy. A particular nucleus

with a particular angular momentum can be characterized by a combination of parameters x and y, provided that the Coulomb, surface, and rotational energies are expressed in the appropriate nuclear terms. In this work, we have used the constants of Myers and Swiatecki[4] to relate the idealized liquid drops of CPS to real nuclei.

Reference 2 gives, as a function of x and y, values for the energies $E_{\min}$ of the stable rotating configurations of equilibrium (lowest-energy rotating states) as well as for the energies E_{sp} of the unstable configurations of equilibrium (saddle-point shapes). It was found that for all values of x, i.e., for all nuclei, the fission barrier vanishes with increasing y. The value of y at which the fission barrier vanishes is a function of x, but it was found that for angular momenta of about $100\hbar$, there are no nuclei that have a finite fission barrier. The limit of $B_f = 0$ is shown in Fig. 1 as a function of angular momentum J for nuclei in the valley of β stability.

Rotating liquid drop equilibrium energies are illustrated for the case of $^{20}Ne + {}^{107}Ag$ in Fig. 2, which gives $E_{\min}$ and E_{sp} as functions of angular momentum. The difference between the two curves, B_f, is also shown. The curve labeled $E^{rr}_{\min}$ is the rotational energy of the undeformed sphere. Note that the fission barrier vanishes at $J \approx 90\hbar$.

B. Deexcitation of compound nuclei

The compound-nucleus deexcitation (with multiple particle emission) program of Blann[5] was modified[1] to include fission competition in the deexcitation process and the calculation was carried out separately for each partial wave involved in a particular reaction. The partial cross sections for the heavy-ion reaction were computed by means of the parabolic-potential approximation of Thomas[6] using a Woods-Saxon real potential. For each value of angular momentum J the calculation was performed for multiple neutron, proton, and α emission, appropriately weighted over spectra of residual excitations as described in Ref. 5, and fission competition was considered at each step of the evaporation process. The evaporation calculations were performed in the Weisskopf-Ewing formalism.[7] The fission competition was calculated from the Bohr-Wheeler[8] expression for fission widths.

The ratio of the fission width to the total width at an angular momentum J was assumed to be given by

$$\frac{\Gamma_f(J)}{\Gamma_{tot}(J)} = N\left[N + 2\sum_{\nu=n,p,\alpha}\int_0^{E'} g_\nu \sigma_\nu(\epsilon)\mu\epsilon\,\rho(E'-\epsilon)d\epsilon\right]^{-1}, \quad (1)$$

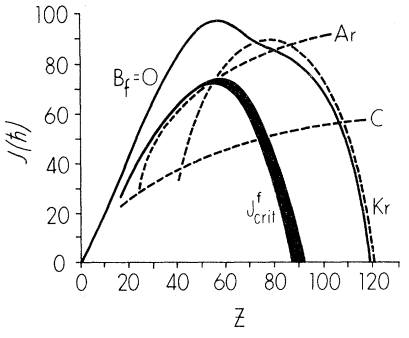

FIG. 1. Predicted limiting angular momenta due to entrance conditions (Ref. 10) and for survival of compound nuclei. Angular momentum is given on the ordinate and target plus projectile atomic numbers are given on the abscissa. The dashed curves represent angular momentum limits for several incident ions. The upper solid curve represents the value of the angular momentum for which the fission barrier is zero according to the rotating liquid drop model of CPS (Ref. 2). The lower solid curve represents the predicted angular momentum limits surviving fission in the deexcitation stages.

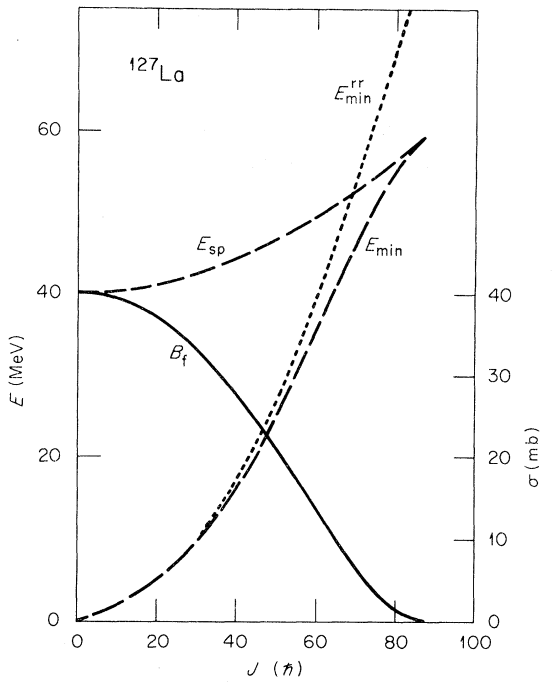

FIG. 2. Liquid drop energies for ^{127}La nuclei according to the rotating drop model of CPS. The ordinate is energy in MeV versus angular momentum on the abscissa. The liquid drop fission barrier (B_f) is shown as the difference between the saddle-point energy of the rotating drop (E_{sp}) and the rotational energy of the rotating drop at equilibrium deformation ($E_{\min}$). For comparison, the rotational energy of a spherical rigid rotor ($E^{rr}_{\min}$) is also shown.

where

$$N = \pi\hbar^2 \int_0^{E''} \rho(E'' - \epsilon)\, d\epsilon ,$$

$$E' = E - E_{\min}(J) - B_\nu ,$$

$$E'' = E - E_{sp}(J) ,$$

and

$$\rho(E) = E^{-2} \exp[2(aE)^{1/2}] .$$

In the above expressions, E is the excitation energy of the compound nucleus, $\rho(E)$ is the level density at excitation energy E, μ is the reduced mass, and a is the level density parameter. In the portion of the Γ_f/Γ_{tot} expression that deals with particle emission g_ν is the statistical factor, $\sigma_\nu(\epsilon)$ is the inverse cross section, and B_ν is the binding energy of evaporating particle ν. Values of B_ν were obtained from Ref. 4, and $\sigma_\nu(\epsilon)$ values were calculated by means of an optical model subroutine. Energy values for the rotating stable equilibrium shapes $E_{\min}(J)$ and for rotating saddle-point shapes $E_{sp}(J)$ were obtained from Ref. 2. A discussion of effects due to changes in angular momentum with particle emission is given in Sec. II D 3.

Figure 3 illustrates the variation of Γ_f/Γ_{tot} with angular momentum for the case of ^{149}Tb obtained from Ar bombardment of ^{109}Ag for first-chance fission. As expected, the variation in Γ_f/Γ_{tot} is strongly correlated with the calculated fission barrier, which is also shown. Curves for partial reaction cross sections for two bombarding energies are also given in Fig. 3. These results are from the parabolic model.[6] It can be seen that at a bombarding energy of 160 MeV, the distribution of partial cross sections is such that fission is not expected to play a significant role in the deexcitation process, while at 288 MeV fission is expected to play a major role.

The computer program used in these calculations is described in detail elsewhere.[9]

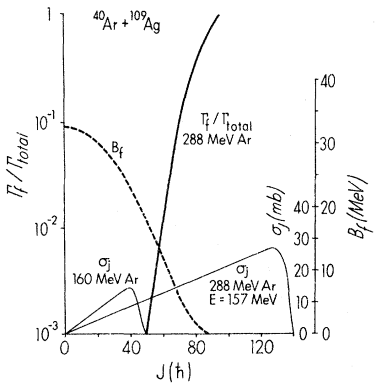

FIG. 3. Fission probabilities and partial wave cross sections for compound nuclei formed by ^{40}Ar bombardment of ^{109}Ag. The left-hand ordinate gives the ratio of fission to total width as a function of angular momentum on the abscissa. The right-hand ordinate gives partial wave cross section on the inside, and fission barrier height on the outside. The fission barrier as a function of angular momentum is given by the dashed curve. The partial wave cross section distributions are given by the thin solid curves. The heavy solid curve represents the ratio of the fission width to the total width as a function of J for first-chance fission.

C. Typical results and implied limits on angular momentum

Results of typical calculations are given in Fig. 4. Consider the center section which gives results for 288 MeV ^{40}Ar incident on ^{109}Ag. The figure shows partial cross sections as a function of angular momentum. The heavy solid line gives the result for the partial cross sections contributing to the total reaction cross section as

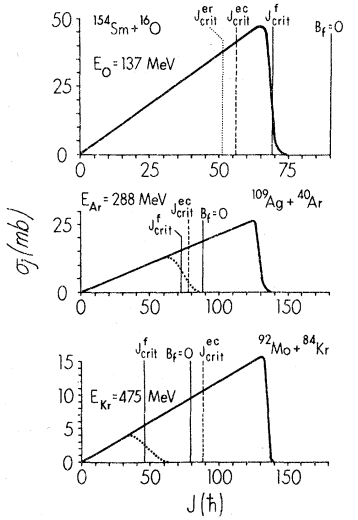

FIG. 4. Partial wave cross sections as a function of angular momentum, and limits on compound nucleus angular momentum. The figure represents three different target-projectile pairs as indicated, and each is at a single bombarding energy. The limits on evaporation residue cross sections due to fission are shown as dotted curves. The equivalent sharp cutoff values are represented by the lines J^f_{crit}. For comparison, the angular momentum for which the liquid drop barrier is zero is also shown ($B_f = 0$). For the case ^{154}Sm + ^{16}O, the experimentally deduced limit of angular momentum from evaporation residue cross sections is indicated by the dotted line J^{er}_{crit} (based on results of Ref. 11). The theoretical limits on compound nucleus angular momentum due to Wilczynski's formulation (Ref. 10) are indicated by the dashed lines J^{ec}_{crit}.

calculated in the parabolic potential approximation. The dotted curve separates the diagram into two areas: on the left of the dotted curve, the compound nuclei are predicted to deexcite by particle emission; on the right of the dotted line, the compound nuclei are expected to fission. Thus, σ_{er} is given by the area to the left of the dotted curve.

When the results are discussed in terms of limiting values of angular momentum, it is necessary to approximate the dotted curve by a vertical line. This was done in Fig. 4, and the vertical lines are labeled J^{f}_{crit}. This is known as the sharp cutoff approximation and implies that an experimental cross section is given by

$$\sigma_{exp} = \pi\lambda^2 \sum_{J=0}^{J_{crit}} (2J+1)T_J ,$$

where T_J is the transmission coefficient and J_{crit} is the critical angular momentum. In comparing our results for J_{crit} with values predicted by others, we shall make use of J^{f}_{crit} in the sharp cutoff approximation with the understanding that calculated results do not, in fact, predict a sharp angular-momentum cutoff.

A further point that needs to be made concerns the area to the right of the dotted curve. One might expect that the area ought to represent the fission cross section σ_f. This would be true only if the total reaction cross section were equal to the compound nucleus cross section. As was discussed earlier, it is possible that the reaction mechanism may be such that it involves a critical angular momentum J^{ec}_{crit} due to entrance conditions which will place a limit on compound nucleus formation. Models for estimating J^{ec}_{crit} will be discussed in Sec. III. Estimates on the basis of one model[10] are given in Figs. 1 and 4. For the $^{109}Ag + ^{40}Ar$ case, J^{ec}_{crit} and J^{f}_{crit} happen to lie close together. Thus both predict equally well the J_{crit} value obtained from σ_{er} measurements. In the other two cases given in Fig. 4, J^{f}_{crit} from our work and J^{ec}_{crit} are further apart. In the case of $^{154}Sm + ^{16}O$, $J^{ec}_{crit} < J^{f}_{crit}$, and thus entrance conditions are expected to determine the cross section for evaporation residue nuclei, as was found to be the case.[11] In the case of $^{92}Mo + ^{84}Kr$, J^{ec}_{crit} is greater than J^{f}_{crit}, and the limit for σ_{er} is expected to be determined by fission competition.

Also indicated in Fig. 4 are the values of angular momentum at which $B_f = 0$. It can be seen that $J(B_f = 0)$ is useful only as an upper limit and that our more realistic calculation predicts considerably lower values of J_{crit}. Thus experimental J_{crit} values should never be compared to $J(B_f = 0)$. This point is also clear in Fig. 1, where entrance condition limits for C, Ar, and Kr projectiles[10] are compared with J^{f}_{crit} limits.

D. Effects of parameter variation and of approximations

1. Level density parameters

There are several parameter variations which should be investigated in determining the reliability of results of these calculations. This is based on the philosophy that it is possible to obtain an indication of the validity of the results on an absolute basis by comparing results from calculations performed with a reasonable span of input parameters. The trends of results with a fixed set of parameters, however, can be quite instructive and valid on a relative basis.

The main uncertainty is in the difference in single-particle level densities for saddle-point and equilibrium-deformed nuclei as determined by a_f/a_ν, which is the ratio of the level density parameter for fission to the parameter for particle emission. For most cases considered in this work, it was assumed that $a_f/a_\nu = 1$; however, effects of varying this ratio are illustrated in Table II. The Fermi gas value of $a_\nu = \frac{1}{8}A$ (where A is

TABLE II. Effects of parameter variation at several bombarding energies for $^{107}Ag + ^{20}Ne$.

a_f/a_ν	B_f/B_f^{ld}	120 MeV (σ_r = 1265.1 mb) σ_{er} (mb)	160 MeV (σ_r = 1697.9 mb) σ_{er} (mb)	200 MeV (σ_r = 1932.4 mb) σ_{er} (mb)
1.0	1.0	1264.8	1425	1236
1.0	1.1	1265.0	1461	1265
1.0	0.9	1264.2	1384	1202
1.1	1.0	1262.5	1149	862
0.9	1.0	1265.1	1614	1603
1.0	1.0	1264.6 [a]	1272 [a]	1093 [a]
1.0	1.0	1264.9 [b]	1518 [b]	1423 [b]

[a] Evaporated particles do not change J.
[b] First chance fission competition only.

the compound nucleus mass number) was used for all calculations of this work. Possible shortcomings of the use of the Bohr-Wheeler expression will be discussed in Sec. IV.

2. *Fission barrier*

Fission barriers used in this work are the liquid drop barriers of CPS.[2] In this subsection we wish to explore the effects of varying the absolute magnitude of the fission barrier. This procedure may be of general use since in certain situations in which our program can be useful it is desirable to consider the height of the fission barrier to be an adjustable parameter. For these purposes, we have included an option in the computer code by means of which it is possible to vary the absolute magnitude of the barrier, while requiring that its dependence on angular momentum be the same as that given by the liquid drop model. This was achieved in practice by changing the ratio B_f/B_f^{ld}, where B_f is the fission barrier used in the calculation, and B_f^{ld} is the fission barrier obtained from the rotating liquid drop model. It was assumed that B_f/B_f^{ld} does not change with angular momentum.

The effect of variation of the ratio B_f/B_f^{ld} is illustrated in Table II for $^{107}Ag+^{20}Ne$, which is typical of the reactions considered in this work. It can be seen that our calculated σ_{er} values are not very sensitive to a 10% variation in the fission barrier. In addition to this typical case, we have calculated the effect of a changing fission barrier for the case of ^{16}O ions incident on ^{197}Au where, presumably, the fissioning nucleus in ^{213}Fr. The fission barrier at zero angular momentum is estimated to be 14.3 MeV,[4] while the corresponding B_f^{ld} value is 8.0 MeV. We have performed the calculation for $B_f=14.3$ MeV and $B_f=8.0$ MeV (at zero angular momentum), as described above, for ^{16}O incident energies of 168 and 100 MeV. At these energies, σ_r was calculated to be 1929 and 711 mb, respectively. For $B_f=B_f^{ld}$, σ_{er} was found to be 220 mb at 168 MeV and 47 mb at 100 MeV. For a fission barrier equal to 14.3 MeV, σ_{er} was 580 mb at 168 MeV and 615 mb at 100 MeV. Thus large changes in the fission barrier (70% in this case) have a large effect on calculated σ_{er} values.

3. *Angular momentum decrease due to particle emission*

The calculations as described in Sec. II B have made use of the so-called s-wave approximation. In this approximation, angular momentum effects are treated identically in compound and residual states, and the initial spin distribution is preserved during the deexcitation process for nuclides not decaying by fission. Thus it is assumed that the outgoing particles do not change the angular momentum distribution.

It is necessary to scrutinize this assumption in order to be certain that a more rigorous treatment of angular momentum coupling in particle emission channels would not give grossly different results. The difficulty in a rigorous treatment of angular momentum is that the computation time for systems typical of this work would be increased by approximately a factor of 1000. Below, we shall describe an approximation in which each evaporated particle decreases the angular momentum of the deexciting nucleus by a fixed amount. This approximation represents the opposite extreme of the s-wave approximation and we feel that there is no better approximation available between it and a rigorous treatment. While one can estimate the average angular momentum removed by the first particle in an emission cascade, there is no simple way to do this for multiple emission and the correct calculation must be performed. Furthermore, even if one knew the over-all average change in angular momentum, this would not be relevant to the question of the change in angular momentum in the particular energy-angular momentum region in which fission and particle emission compete (see Fig. 3).

An important observation is that fission competition decreases rapidly with decreasing excitation in the energy-angular momentum region involved in this work [see Eq. (1)]. At excitations which are high with respect to rotational energies, angular momentum coupling in the exit channels is weak, and the s-wave approximation becomes poor only in the final stages of the evaporation cascade, when strong coupling occurs in the exit channels. Fission competition, however, plays a role primarily in the early stages of the evaporation cascade, before the approximation becomes relatively poor. Since in this work we are exploring the role of fission enhancement due to high angular momenta rather than angular momentum effects on particle evaporation, the s-wave approximation is acceptable. Angular momentum effects in the deexcitation of compound nuclei have been treated earlier, and effects of changes in J during the evaporation cascade are illustrated in the contour diagrams of Ref. 12.

It is, however, instructive to have an upper-limit indication of the changes that might result from a more rigorous treatment of this problem. A simple way to accomplish this is to perform a calculation in which each particle emitted removes an amount of angular momentum characteristic of a maximum value which is expected for strong coupling of partial waves that have significant

TABLE III. Cross sections and limiting angular momenta for selected heavy-ion reactions.

Projectile	Target	E_{lab} (MeV)	σ_r (mb)	σ_{er} (mb)	J^f_{crit} ($\hbar$)	ΔJ ? [a]	Comments
^{16}O	^{154}Sm	132	1686	1670	66	Yes	
		137	1745	1445	62	No	979 expt σ_{er}
		137	1745	1710		Yes	
^{12}C	^{158}Gd	121	1928	1924	60	Yes	
		126	1977	1902	61	No	1096 expt σ_{er}
		126	1977	1970		Yes	
^{11}B	^{159}Tb	110	2038	2036	57	Yes	
		115	2086	2066	58	No	980 expt σ_{er}
		115	2086	2083		Yes	
^{20}Ne	^{150}Nd	139	1416	1394	68	Yes	
		144	1487	1165	62	No	
		144	1487	1435		Yes	
^{12}C	^{58}Ni	98	1655	1651		No	
		120	1737	1682		Yes	
		150	1794	1530		Yes	
		180	1821	1250	53	No	
		180	1821	1404	55	Yes	
^{16}O	^{27}Al	100	1512	1030	30	No	
		100	1512	1180	33	Yes	
		130	1569	754	30	No	
		130	1569	950	33.5	Yes	
		160	1590	650	31	No	
		160	1590	840	35	Yes	
^{16}O	^{65}Cu	80	1330	1330	...	No	
		100	1559	1359	...	No	
		110	1636	1626	53	No	
		110	1636	1633	53	Yes	
		136	1771	1400	54	No	
		136	1771	1625	58	Yes	
		168	1863	1160	54	No	
		168	1863	1410	60	Yes	
		243	1950	1123	64	Yes	
^{16}O	^{107}Ag	98	1310	1310	...	No	
		112	1515	1515	...	No	
		133	1729	1721	...	Yes	
		133	1729	1700	64	No	
		168	1947	1710	72	Yes	
		168	1947	1530	68	No	
^{20}Ne	^{27}Al	87	1345	1310	33	No	
		87	1345	1310	33	Yes	
		107	1465	1082	33	No	
		107	1465	1220	35	Yes	
		127	1536	880	33	No	
		127	1536	1041	35.5	Yes	
		143	1572	780	32.5	No	
		143	1572	960	36	Yes	
		210	1636	600	34.5	No	
				754	39	Yes	
^{20}Ne	^{107}Ag	100	872	872	...	No	
		100	872	872	...	Yes	
		140	1518	1406	64	No	
		140	1518	1480	66	Yes	
		165	1735	1213	65	No	
		165	1735	1426	70	Yes	

TABLE III *(Continued)*

Projectile	Target	E_{lab} (MeV)	σ_r (mb)	σ_{er} (mb)	J^f_{crit} ($\hbar$)	ΔJ? [a]	Comments
		210	1974	1850	66	No	
		210	1974	1194	73	Yes	
^{40}Ar	^{58}Ni	140	586	586	...	No	
		200	1301	823	58	No	
		288	1753	593	59	No	
		288	1753	754	67	Yes	
^{40}Ar	^{109}Ag	160	389	389	59	No	
		200	1037	600	61.5	No	
		200	1037	730	68	Yes	
		226	1322	534	62	No	
		240	1447	500	62	No	
^{40}Ar	^{109}Ag	288	1771	430	63	No	
		288	1771	581	73	Yes	
		288	1771	797	78	Yes	$a_f/a_\nu = 0.75$
		288	1771	610	75	Yes	$B_f = 1.2B_f^{ld}$
		320	1925	435	69	No	
		320	1925	545	74	Yes	
^{40}Ar	^{165}Ho	288	1598	140	11	Yes	
^{84}Kr	^{10}B	800	1930	1930	≥51	Yes	
^{84}Kr	^{27}Al	605	1755	1135	71	Yes	
^{84}Kr	^{65}Cu	330	424	422	58	No	
		330	424	424	58	Yes	
		475	1412	370	65	No	
		475	1412	450	71	Yes	
		605	1856	326	68	No	
		605	1856	400	75	Yes	
^{84}Kr	^{92}Mo	340	2.4				
		350	84	78	34	No	
		475	1123	123	44	No	
		605	1709	121	51	No	
		475		140	47	Yes	
^{84}Kr	^{127}I	475	1069	9	13	Yes	

[a] For ΔJ = No, evaporation of particles does not change the angular momentum of the residual nucleus; for ΔJ = Yes, particle evaporation decreases the angular momentum as described in Sec. II D 3.

transmission coefficients and for energies characteristic of evaporation. We have done such a calculation, and assumed that each neutron emitted decreased J by $2\hbar$, and each proton by $3\hbar$. The logic by which this was accomplished in the computer code made it simplest to assume that nuclides populated by α decay have an angular momentum that is $10\hbar$ lower than that of the parent nuclide. Reference to the curves of average angular momentum removed by α evaporation in Ref. 13 indicate that this is a reasonable value. We feel that the results of a rigorous calculation must lie between the limits given by the two sets of calculations described in this work. Our results are summarized and compared in Table III.

Several of the results presented in Sec. IV and in Table III are given both with and without the option of changing angular momentum following particle emission. The magnitude of the effect is also illustrated in Table II for ^{107}Ag+^{20}Ne. On the whole, it was found that calculated σ_{er} values were in better agreement with experimental results when the emitted particles were assumed to remove angular momentum from the emitting nuclide. The large differences between the calculation with and without the angular momentum option indirectly indicates the importance of considering multiple chance fission for these systems. A more direct effect of first-chance relative to multiple-chance fission in competition with particle-emission is

also shown in Table II. For example, for the 200 MeV ^{20}Ne bombardment of ^{107}Ag, $\sigma_f = 509$ mb for first-chance fission and $\sigma_f = 694$ for multiple-chance fission.

III. ENTRANCE CONDITION LIMITS ON COMPOUND NUCLEUS CROSS SECTIONS

In our calculation, we have not considered the question of whether or not a compound nucleus will be formed, or whether some limit imposed by entrance conditions or some preequilibrium phenomenon will restrict the range of impact parameters that can result in the formation of a compound nucleus. Rather, we have asked the question: "If compound nuclei are formed with the predicted J distribution, what part of the population can be expected to survive fission deexcitation?"

Several approaches have been taken in an attempt to answer the question of limits due to entrance conditions. These efforts are similar to each other in that they all consider a potential energy surface based on a surface attractive term and Coulomb plus centrifugal repulsive terms. The crucial questions in such models are the rate of collective nuclear matter outflow in the neck region of the colliding target plus projectile relative to the interaction time in the reaction channel, the manner of collective rotation of the fusing systems, and the friction or nuclear viscosity for the interacting nuclei. The degree of outflow determines the change in surface area and therefore the attractive (surface) potential. The viscosity determines the energy dissipation and plays a role in determining whether or not the two nuclei will stick together. A formulation in which a somewhat arbitrary rate of flow to ellipsoidal shapes was assumed was offered by Kalinkin and Petkov in 1964.[14] More recently Wilczynski[10] described a formulation in which the surface attractive potential of two spheres at 50% density overlap (for which maximum attractive force results) was assumed; Bass has calculated potentials as a function of the overlap.[15] Predictions of the model formulated by Wilczynski for Ne- and Kr-induced reactions are shown in Fig. 1 where they are compared with our calculations for J^{f}_{crit} and with $J(B_f = 0)$. It must be remembered that the fission cross section (for compound nucleus fission only) must be added to the σ_{er} value before J^{cn}_{crit} values can be obtained for comparison with entrance condition models which predict compound nucleus cross sections rather than evaporation residue cross sections.

As was suggested earlier, angular momentum limits imposed by contact configuration considerations and limits imposed by the fission model are not mutually exclusive when applied to measurements of evaporation residue nuclei. This point, which was discussed in Sec. II C, is illustrated in Fig. 4. If J^{ec}_{crit} is the critical angular momentum associated with contact configuration limitations from Wilczynski's model, and J^{f}_{crit} is the fission-imposed angular momentum limit, σ_{er} values are expected to be determined by whichever value of J_{crit} is smaller. In the top part of the figure J^{ec}_{crit} is smaller than J^{f}_{crit} and contact configuration considerations dominate. In the bottom part of the figure $J^{f}_{crit} < J^{ec}_{crit}$, and σ_{er} will be determined by the extent of fission competition. In the center part of the figure $J^{f}_{crit} \approx J^{ec}_{crit}$, and both models are expected to predict σ_{er} equally well.

Evidence of the importance of contact configuration limits on σ_{er} was shown in the work of Zebelman and Miller.[11] Their results for the formation of the compound nucleus ^{170}Yb with ^{11}B, ^{12}C, and ^{16}O projectiles are summarized in Table III. J^{er}_{crit} values deduced from these bombardments appear to be projectile-dependent. Our calculated J^{f}_{crit} values are also given in the table.

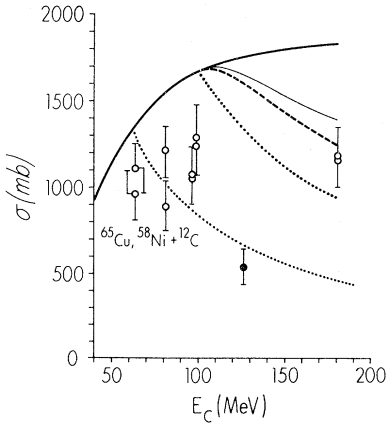

FIG. 5. Experimental evaporation residue excitation functions versus calculated evaporation residue and fusion limits for ^{12}C-induced reactions on ^{58}Ni and ^{65}Cu. The open points represent experimental counter telescope results from Ref. 16. The closed point is from track detector measurements of Ref. 16. The lower dotted curve is the fusion limit calculated by Wilczynski's formulation (Ref. 10). The upper dotted curve is the authors' interpretation of the Tsang-Swiatecki (Ref. 21) and Bass limit (Ref. 15) assuming high viscosity. The thin solid curve is a calculated limit to the evaporation residue cross section based on the rotating liquid drop model, with evaporated particles removing some angular momentum. The dashed curve is the same as the thin solid curve, but with evaporated particles removing no angular momentum (see Sec. II D 3). The heavy solid curve is the total reaction cross section calculated with the parabolic model (Ref. 6).

IV. CALCULATED AND EXPERIMENTAL RESULTS AND DISCUSSION

Calculated results for several target-projectile combinations and several bombarding energies are given in Table III. It may be noted that the fission-imposed limit on J, J^{f}_{crit}, results in J values which increase slowly with increasing bombarding energy for a given compound nucleus. This is qualitatively consistent with recent experimental results.[16,17]

Several sets of experimental σ_{er} values are shown in Figs. 5–8. Results were measured with mica or lexan track detectors and with counter telescopes. For the case of $^{109}Ag+^{40}Ar$ (Fig. 8), fission cross sections were also measured. This permitted points corresponding to $\sigma_{cn}=\sigma_{er}+\sigma_{f}$ to be plotted in Fig. 8. Several sets of calculated results are presented in Figs. 5–8. The calculated limit on σ_{er} due to fission competition is in reasonably good agreement with experimental results for the $^{27}Al+^{16}O$ and the $^{20}Ne+^{107}Ag$ systems as well as for the ^{40}Ar bombardment and for the highest energy measurement in the $^{65}Cu+^{12}C$ case. Agreement is unsatisfactory for the $^{107}Ag+^{16}O$ system. Limits to σ_{er} due to fission competition are shown for both the s-wave approximation and for the calculation described in Sec. IID 3 in which it is assumed that particle emission alters the angular momentum of the residual nuclide.

Several comments should be made as to the applicability of the simple Bohr-Wheeler model to these reactions. The Bohr-Wheeler approach assumes an equilibrium in all degrees of freedom, consisting of intrinsic degrees of freedom and of fission degrees of freedom. Computation of different level densities due to coupling of rotational degrees of freedom to intrinsic and fission modes has not been treated in this work. The importance of such considerations has recently been discussed by Bjørnholm, Bohr, and Mottelson[18] and by Freiesleben, Britt, and Huizenga.[19]

In addition, the lifetimes expected for such highly excited systems are quite short with respect to

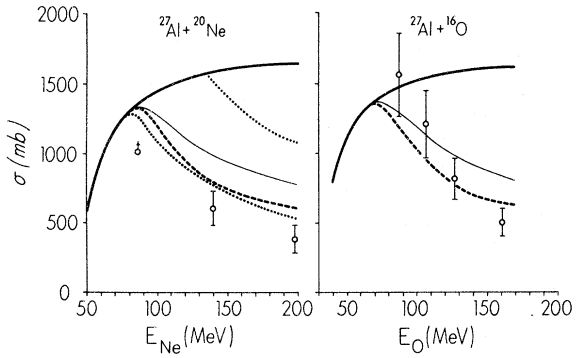

FIG. 6. Comparison of experimental evaporation residue cross sections for $^{20}Ne+^{27}Al$ and $^{16}O+^{27}Al$ with calculated fusion and evaporation residue cross sections. Experimental results are from Ref. 22. Calculated results are as in Fig. 5. Recent results indicate that the experimental points at higher energies may have to be revised upward (Ref. 23).

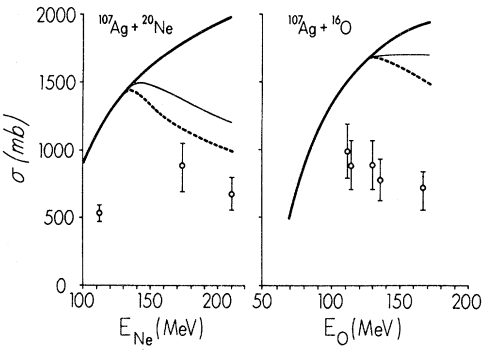

FIG. 7. Comparison of experimental evaporation residue excitation functions with calculated evaporation residue and fusion limits for ^{20}Ne and ^{16}O induced reactions on ^{107}Ag (Ref. 16). The curves have the same meaning as in Figs. 5 and 6.

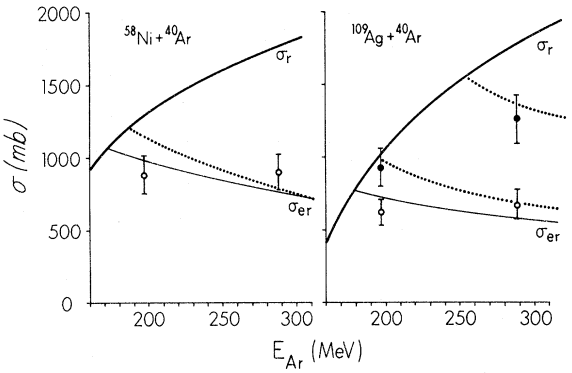

FIG. 8. Experimental and calculated fusion cross section limits for ^{40}Ar bombardments of ^{58}Ni and ^{109}Ag. The heavy solid curves represent total reaction cross sections calculated with the parabolic model (Ref. 6). The open points represent experimental evaporation residue cross sections. The solid points for the ^{109}Ag target represent the sum of evaporation residue plus fission cross sections. The lower dotted curve represents the limiting cross section due to the contact configuration according to Ref. 10; the upper dotted curve represents the limit according to a similar model described in Sec. IV (Ref. 21). The thin solid curve represents the cross section limit predicted for the evaporation residues due to fission deexcitation as calculated in this work. This figure is reproduced from Ref. 24.

equilibration times. Precompound particle emission may well be present in the early deexcitation stages, in which case there would be less fission competition than predicted by the simple treatment of this work, or for that matter, by a more rigorous evaporation-fission-competition calculation in which particles other than neutrons, protons, and α particles are also considered (see, for example, Ref. 20). It is likely that during the process which leads from the target and projectile nuclei in their ground states to a compound nucleus that involves many particle-hole excitations, the system passes through a stage in which the number of particle-hole excitations is less than the number at equilibrium. At such a stage it is reasonable to expect preequilibrium particle emission. The discrepancies between calculated and experimental results in this work are in a direction consistent with a possible preequilibrium effect, i.e., fission is overestimated at high excitations.

Comparisons with limits due to entrance conditions are somewhat tenuous for those systems for which σ_f has not been measured in addition to σ_{er}. As was stated earlier, $\sigma_{cn}=\sigma_{er}+\sigma_f$, and entrance condition models predict the compound nucleus cross section. Nonetheless, fission should be small for some of the systems shown in Figs. 5–8, in particular at the lower energies.

Some of the implicit assumptions in the entrance condition models have been discussed in Sec. III. The J^{cc}_{crit} values determined from these models depend upon the manner in which the moment of inertia is computed for the target plus projectile, and on the type of relative rotational motion between these two bodies. Limits calculated by Wilczynski's formulation for a collision in which there is no collective rotation about a common two-body axis are shown in Figs. 5–8. An upper limit which would result from a motion of one body rolling around the other with zero relative surface velocity is also shown in some of the Figs. 5–8 as the higher calculated σ_{cn} values due to a contact configuration formulation.[21] The upper cross section limits are approximately twice the values given by a formulation with no relative rotational energy about a common two-body axis. There does not seem to be a general consistency of agreement between compound nucleus limits calculated by either of the two ways discussed above (choice of moment of inertia in contact configuration models) and the experimental results. Again it should be emphasized that σ_{er} is at best a lower limit to the σ_{cn} with which comparisons should be made. In the case of $^{109}Ag+^{40}Ar$, σ_{cn} was measured at 288 MeV. In this case, the σ_{ec} for the "rolling" mode of relative motion is in reasonable agreement with the experimental result.

In most of the cases shown, the predicted σ_{er} values based on the fission competition model are in reasonable agreement with experimental trends and cross sections. Many more data of a survey nature, involving both σ_{er} and σ_f measurements, are needed to determine the validity of the models under discussion in this work.

V. CONCLUSIONS

We have explored a model which predicts limits to σ_{er} in heavy-ion reactions due to consequences of lowering the fission barrier at high angular momentum states. Predictions of this model have been compared with σ_{cn} limits due to entrance conditions by use of several illustrative examples. Predictions of models of both types have been compared with experimental results. The fission limit is consistent with experimental σ_{er} results in many cases. We conclude that many precise measurements of σ_{er} and σ_f as a function of target, projectile, and energy are needed before conclusions can be drawn as to the extent of usefulness of the fission deexcitation model in predicting σ_{er} values. The model has been shown to predict J^{l}_{crit} values which slowly increase with increasing excitation energy in agreement with limited experimental observations.

---

*Operated by Union Carbide Corporation for the U.S. Atomic Energy Commission.

†Supported in part by the U.S. Atomic Energy Commission.

[1]M. Blann and F. Plasil, Phys. Rev. Lett. 29, 303 (1972).

[2]S. Cohen, F. Plasil, and W. J. Swiatecki, Ann. Phys. (N.Y.) 82, 557 (1974).

[3]S. Cohen and W. J. Swiatecki, Ann. Phys. (N.Y.) 22, 406 (1963).

[4]W. D. Myers and W. J. Swiatecki, Ark. Fys. 36, 343 (1967).

[5]M. Blann, Nucl. Phys. 80, 223 (1966).

[6]T. D. Thomas, Phys. Rev. 116, 703 (1959).

[7]V. Weisskopf and D. H. Ewing, Phys. Rev. 57, 472 (1940).

[8]N. Bohr and J. A. Wheeler, Phys. Rev. 56, 426 (1939).

[9]M. Blann and F. Plasil, ALICE: A Nuclear Evaporation Code, U.S. Atomic Energy Commission Report No. COO-3494-10, 1973 (unpublished).

[10]J. Wilczynski, in *Proceedings of the Third International Atomic Energy Symposium on the Physics and Chemistry of Fission, Rochester, 1973* (International Atomic Energy Agency, Vienna, Austria, 1974), Vol. II, p. 269.

[11]A. M. Zebelman, K. Beg, Y. Eyal, G. Jaffe, D. Logan, J. Miller, A. Kandil, and L. Kowalski, in *Proceedings of the Third International Atomic Energy Symposium on the Physics and Chemistry of Fission, Rochester, 1973* (see Ref. 10), Vol. II, p. 335.
[12]M. Blann, Phys. Rev. 157, 860 (1967).
[13]T. D. Thomas, Annu. Rev. Nucl. Sci. 18, 343 (1968).
[14]B. N. Kalinkin and I. Zh. Petkov, Acta Phys. Pol. 25, 265 (1964).
[15]R. Bass, Phys. Lett. 47B, 139 (1973).
[16]J. B. Natowitz, Phys. Rev. C 1, 623, 2157 (1970); J. B. Natowitz, E. T. Chulick, and M. N. Namboodiri, Phys. Rev. C 6, 2133 (1972).
[17]J. Galin, D. Guerreau, M. Lefort, and X. Tarrago, Phys. Rev. C 9, 1018 (1974), and other references listed therein.
[18]S. Bjørnholm, A. Bohr, and B. R. Mottelson, in *Proceedings of the Third International Atomic Energy Symposium on the Physics and Chemistry of Fission, Rochester, 1973* (see Ref. 10), Vol. I, p. 367.
[19]H. Freiesleben, H. C. Britt, and J. R. Huizenga, in *Proceedings of the Third International Atomic Energy Symposium on the Physics and Chemistry of Fission, Rochester, 1973* (see Ref. 10), Vol. I, p. 447.
[20]M. Blann, Phys. Rev. 133, B707 (1964).
[21]Chin-Fu Tsang and W. J. Swiatecki, private communication.
[22]L. Kowalski, J. C. Jodogne, J. M. Miller, Phys. Rev. 169, 894 (1968).
[23]L. Kowalski, R. L. Kozub, D. Logan, N. H. Lu, and J. M. Miller (unpublished).
[24]H. H. Gutbrod, F. Plasil, H. C. Britt, B. H. Erkkila, R. H. Stokes, and M. Blann, in *Proceedings of the Third International Atomic Energy Symposium on the Physics and Chemistry of Fission, Rochester, 1973* (see Ref. 10), Vol. II, p. 309.